Supporting Information

High-depth fluorescence imaging using a two-photon FRET system for mitochondrial pH in live cells and tissues

Min Jung Chang,[a] Kyutae Kim,[b] Kyun Seob Park,[b] Ji Su Kang,[c]
Chang Su Lim,*[c] Hwan Myung Kim,*[c] Chulhun Kang*[b] and Min Hee Lee*[a]

[a]*Department of Chemistry, Sookmyung Women's University, Seoul, 04310, Korea*
[b]*The School of East-West Medical Science, Kyung Hee University, Yongin, 17104, Korea*
[c]*Department of Chemistry, Ajou University, Suwon, 16499, Korea*

*Corresponding authors: cslim8112@gmail.com (C. S. Lim); kimhm@ajou.ac.kr (H. M. Kim), kangch@khu.ac.kr (C. Kang); minheelee@sookmyung.ac.kr (M. H. Lee)

Contents

1. Materials and instrumentation

All fluorescence and UV/Vis absorption data were collected using RF-6000 (Shimadzu Corporation, Kyoto, Kyoto Prefecture, Japan) and UV-2600 (Shimadzu Corporation, Kyoto, Kyoto Prefecture, Japan) spectrophotometers, respectively. ^{1}H and ^{13}C NMR spectra were collected in $CDCl_3$ (Cambridge Isotope Laboratories, Cambridge, MA) on Varian INOVA 400 MHz spectrometers. Silica gel 60 (Merck, 0.063 - 0.2mm) was used for column chromatography. Analytical thin layer chromatography was performed using Merck60 F_{254} silica gel (precoated sheets, 0.25 mm thick). All reactions were carried out under nitrogen atmosphere. All reagents including piperazine, acetonitrile, metals such as chloride salts of metal ions, tetrabutylammonium (TBA) salts of anions, thiols such as cysteine (Cys), homocysteine (Hcy), glutathione (GSH) generation and other chemicals for synthesis, buffer solutions were purchased from Aldrich, Alfa, TCI and used as received. All solvents were analytical reagents. DMSO for spectroscopic experiments was HPLC reagent without fluorescent impurity and water was deionized water.

2. UV/Vis absorption and fluorescence spectroscopic methods

2.1. Spectroscopic measurements

Stock solution of synthetic compounds were prepared in DMSO. Different pH buffer solutions were prepared by using literature procedures.[1] Stock solutions of TBA salts of anions and chloride salts of metal ions were prepared in CH_3CN and HPLC grade water, respectively. Stock solutions of reactive oxygen species were prepared by using literature procedures.[2] Briefly, H_2O_2, tert-butylhydroperoxide (HOO^tBu) and hypochloride (NaOCl) were delivered from 35%, 70%, and 11–14% aqueous solutions, respectively. Hydroxyl radical ($^{\bullet}OH$) and tert-butoxy radical ($^tBuO^{\bullet}$) were generated by the reaction of 10 mM $Fe(ClO_4)_2$ with 10 mM H_2O_2 or HOO^tBu, respectively. Stock solutions of thiols were prepared in 20 mM pH 7.4 PBS buffer solution. Samples for absorption and emission measurements were contained in quartz cuvettes (4 mL volume). Excitation was provided at 410 and 560 nm with excitation and emission slits widths being set at 5 nm and 3 nm.

2.2. Measurement of energy transfer efficiency (ETE)

The energy transfer efficiency (ETE) was calculated by using the equation:

$$ETE\ (\%) = \left(1 - \frac{Abs_1(410\ nm) \cdot F_1}{Abs_2(410\ nm) \cdot F_2}\right) \times\ 100$$

Abs_1 and Abs_2 are the absorbances of **1** and **2** at 410 nm, and F_1 and F_2 are the emission intensities of **1** and **2** upon excitation at 410 nm, respectively.[3-5] The value of ETE was obtained as 98.1%. Also, the antenna effect was 0.12, as calculated by dividing the area of emission from **1** upon excitation of 410 nm by that collected from the excitation of **3** at 560 nm. Therefore, the decrease at 550 nm can be attributed to the FRET from naphthalimide moiety to rhodamine moiety of **1** with an energy transfer efficiency of 98.1 %, and the increase at 590 nm can be attributed to an antenna effect.[3-5]

3. Cell culture and confocal microscopic methods

3.1. Cell culture

A human cervical cancer cell line (HeLa) was cultured in Dulbecco's modified Eagle's medium (DMEM) supplemented with 10% FBS (WelGene), penicillin (100 units/mL), and streptomycin (100 μg/mL). Two days before imaging, the cells were passed and plated on glass-bottomed dishes (MatTek). All the cells were maintained at 37 °C in a humidified atmosphere consisting of 5/95 (v/v) CO_2/air. For labeling, the growth medium was removed and replaced with DMEM without FBS. The cells were treated and incubated with 5.0 μM of **1** at 37 °C under 5% CO_2 for the specific incubation time associated with a given experiment. The cells were washed three times with phosphate buffered saline (PBS, Gibco). Cell images were then recorded using a confocal microscope (Leica, model TCS SP2). Other information is available in the figure captions.

3.2. Measurement of two-photon cross section

The two-photon cross section (δ) was determined by using femtosecond (fs) fluorescence measurement technique as described.[6] Probe **1** (5 μM) was dissolved in pH 3.0 and 9.0 universal buffer solution containing 10 % DMSO (v/v) and the two-photon induced fluorescence intensity was measured at 720-940 nm by using rhodamine 6G as the reference, whose two-photon property has been well characterized in the literature.[7] The intensities of the two-photon induced fluorescence spectra of the reference and sample emitted at the same excitation wavelength were determined. The TPA cross section was calculated by using $\delta = \delta_r(S_s\Phi_r\phi_r c_r)/(S_r\Phi_s\phi_s c_s)$: where the subscripts s and r stand for the sample and reference molecules. The intensity of the signal collected by a CCD detector was denoted as S. Φ is the fluorescence quantum yield. ϕ is the overall fluorescence collection efficiency of the experimental apparatus. The number density of the molecules in solution was denoted as c. δ_r is the TPA cross section of the reference molecule.

3.3. One- and Two-photon fluorescence microscopy

One- and two-photon microscopy (OPM and TPM) images of SCa1-IREF labelled cells and tissues were obtained with spectral confocal and multiphoton microscopes (Leica TCS SP8 MP) with × 40 oil objectives, numerical aperture (NA) = 1.30. The two-photon fluorescence microscopy images were obtained with a DMI6000B Microscope (Leica) by exciting the probes with a mode-locked titanium-sapphire laser source (Mai Tai HP; Spectra Physics, 80 MHz pulse frequency, 100 fs pulse width) set at wavelength (OPM) 552 and (TPM) 860 nm. Output power for OPM and TPM imaging were 20 and 2540 mW, respectively, which corresponded to approximately 2.2 mW average power in the focal plane. Images were captured at 550-700 nm range, internal PMTs were used to collect the signals in an 8 bit unsigned 512 × 512 pixels at 400 Hz scan speed. Ratiometric image processing and analysis was carried out using MetaMorph software.

3.4. Co-localization experiments

Co-localization experiments were conducted by co-staining the HeLa cells and appropriate combinations of **1** (2 μM), MitoTracker Green (0.5 μM), LysoTracker Green (0.3 μM) and ERTracker Green (0.3 μM) for 30 min. TPM and OPM images were obtained by collecting the emissions at 585–615 (**1**), 505–530 nm (Tracker Green), respectively. The two different detection windows for **1** were adopted upon requirement for colocalization

experiments. The background images were corrected, and the distribution of pixels in the OPM and TPM images acquired in the green and red channels, respectively, was compared by using scatter gram. The Pearson's co-localization coefficients (PCC) were calculated by using AutoQuant X2 program.

4. Synthesis of compounds 1-3

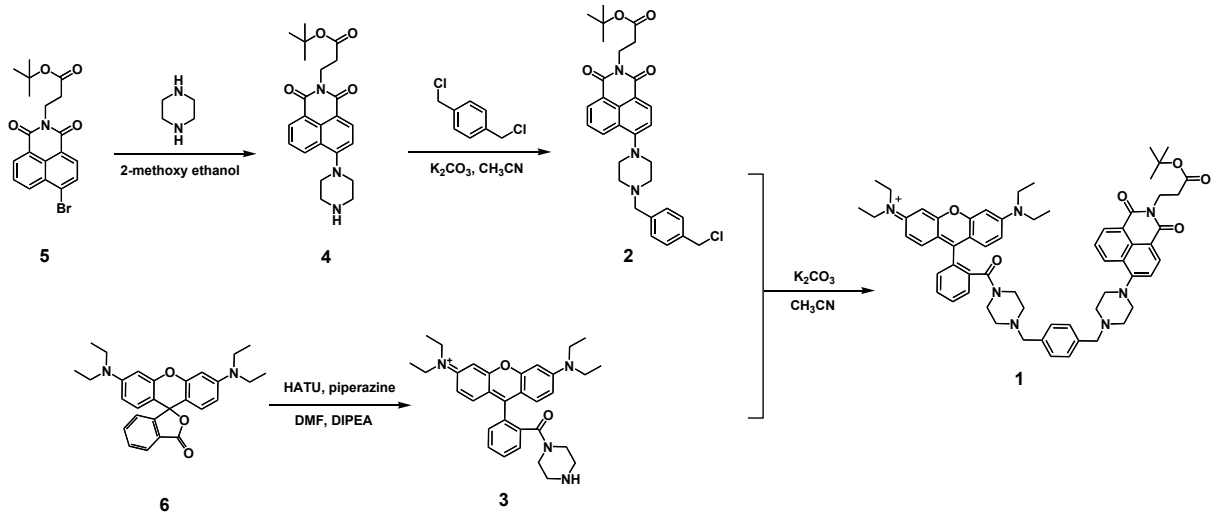

Scheme S1. Synthetic routes for **1**-**3**.

Precursors **2** and **3** were prepared according to the previously published procedures.[8,9]

*Synthesis of Probe **1***

Precursors **2** (0.2 g, 0.3 mmol) and **3** (0.2 g, 0.3 mmol) were stirred in the presence of K_2CO_3 (0.1 g, 0.7 mmol) as a base in acetonitrile (CH_3CN). After refluxing for 20 h under nitrogen atmosphere, the solvent was evaporated under vacuum. The crude product was dissolved in dichloromethane (DCM), thoroughly washed with H_2O, dried over Na_2SO_4. After evaporating solvent, the crude product was purified by silica gel column chromatography using DCM and methanol (v/v, 55:1) as the eluent. This gave product **1** as a dark pink solid in 52% yield (0.18 g). HR-ESI-MS *m/z* calcd (M^+) 1022.54658, found 1022.55406 (M^+). ^{1}H NMR ($CDCl_3$, 400 MHz): δ 8.53 (d, 1H, J = 7.2 Hz); 8.47 (d, 1H, J = 8.0 Hz); 8.41 (d, 1H, J = 8.4 Hz); 7.69-7.65 (m, 3H); 7.55-7.54 (m, 1H); 7.35-7.29 (m, 3H); 7.24 (d, 4H, J = 9.2 Hz); 7.18 (d, 1H, J = 8.0 Hz); 6.93 (d, 2H, J = 9.2 Hz); 6.77 (s, 2H); 4.41 (t, 2H, J = 7.6 Hz); 3.65-3.58 (m, 10H); 3.43-3.30 (m, 10H); 2.77 (s, 4H); 2.67 (t, 2H, J = 7.6 Hz); 2.32 (s, 2H); 2.26 (s, 2H); 1.42 (s, 9H); 1.33 (t, 12H, J = 7.0 Hz) ppm. ^{13}C NMR ($CDCl_3$, 100 MHz): δ 170.6, 167.3, 164.2, 163.7, 157.7, 156.2, 156.0, 155.6, 136.8, 136.4, 135.5, 132.6, 132.1, 131.1, 130.6, 130.1, 130.0, 129.8, 129.2, 129.1, 127.6, 126.0, 125.6, 122.9, 116.1, 114.8, 114.0, 113.7, 96.2, 80.6, 62.6, 62.5, 53.2, 53.0, 52.3, 47.6, 46.0, 41.8, 36.0, 33.9, 28.0, 12.6 ppm.

5. ^{1}H NMR, ^{13}C NMR and HR-ESI-MS data

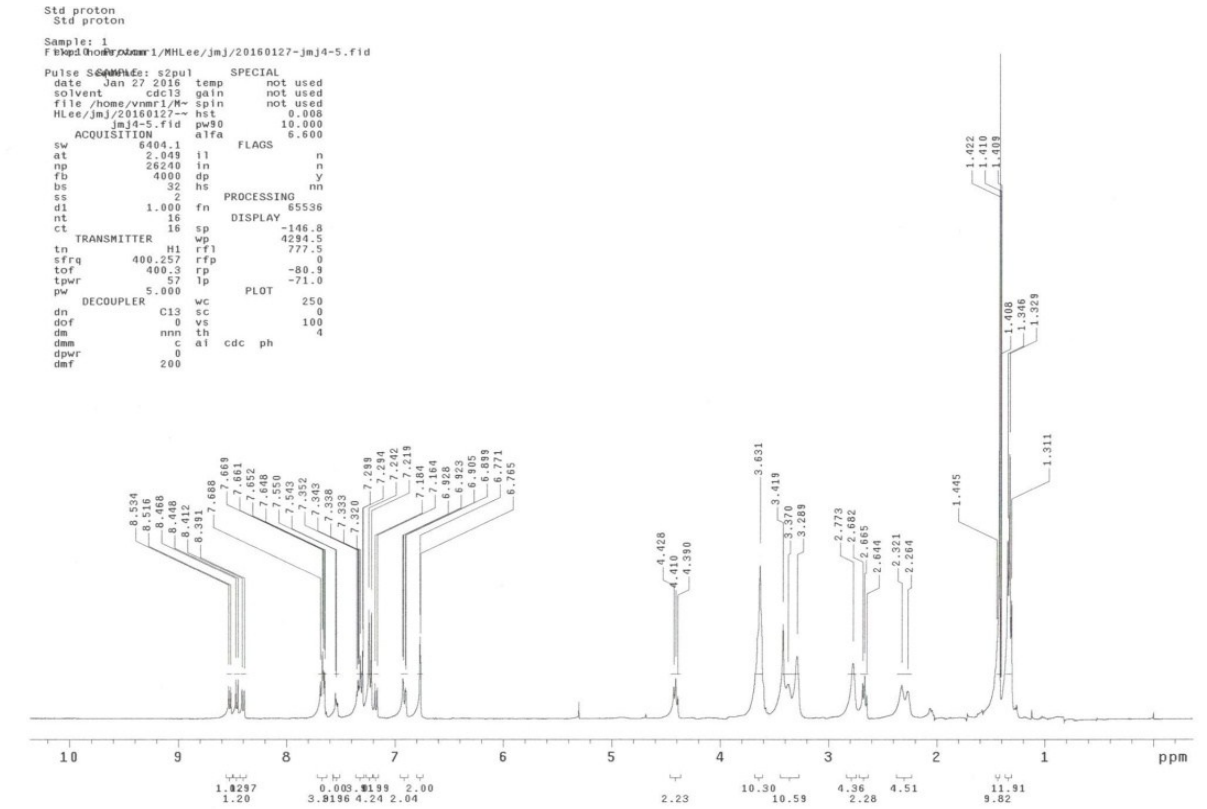

Figure S1. ^{1}H NMR spectrum of **1** in $CDCl_3$.

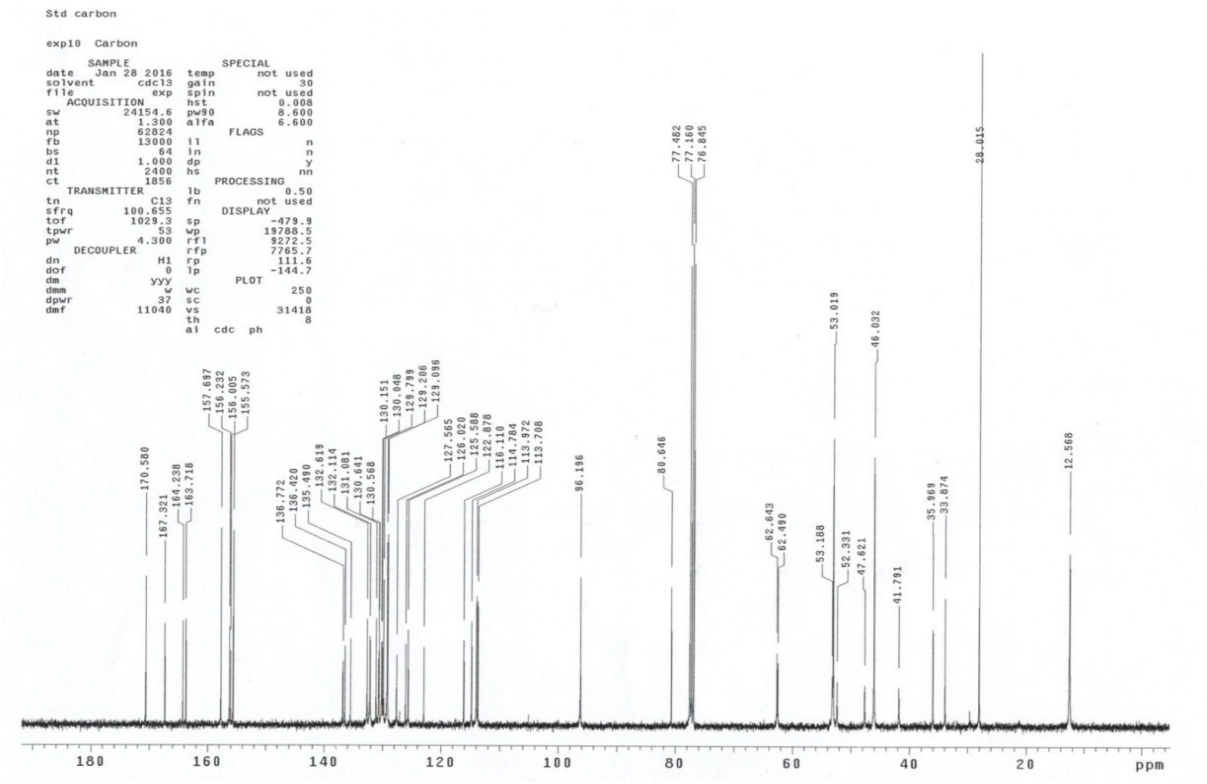

Figure S2. ^{13}C NMR spectrum of **1** in $CDCl_3$.

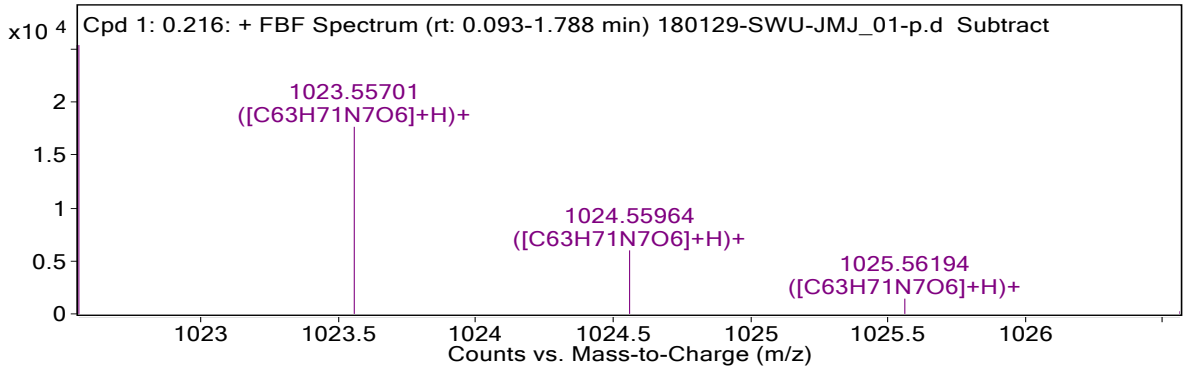

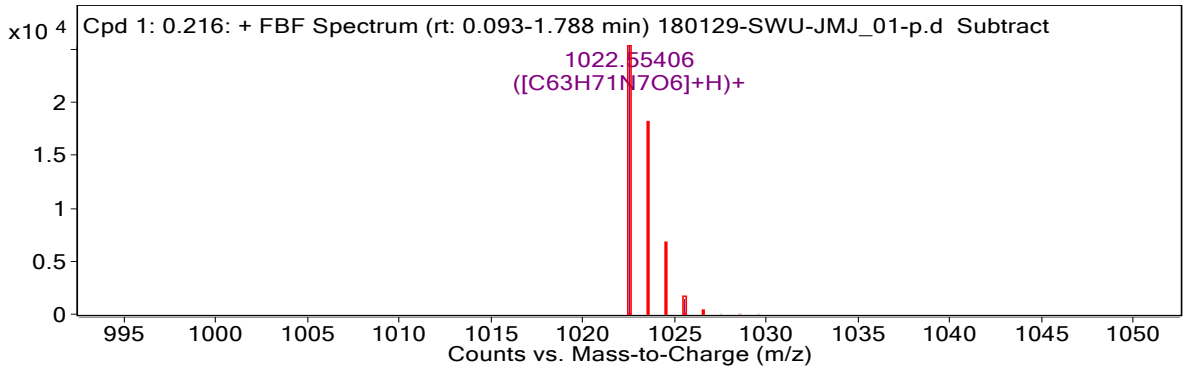

MS Spectrum Peak List

m/z	z	Abund	Formula	Ion
1022.55406	1	25362.68	C63H71N7O6	(M+H)+
1023.55701	1	17650.47	C63H71N7O6	(M+H)+
1024.55964	1	5992.99	C63H71N7O6	(M+H)+
1025.56194	1	1436.9	C63H71N7O6	(M+H)+
1026.56388	1	249.09	C63H71N7O6	(M+H)+

Figure S3. HR-ESI-MS spectrum of **1**.

6. Additional spectroscopic and imaging data

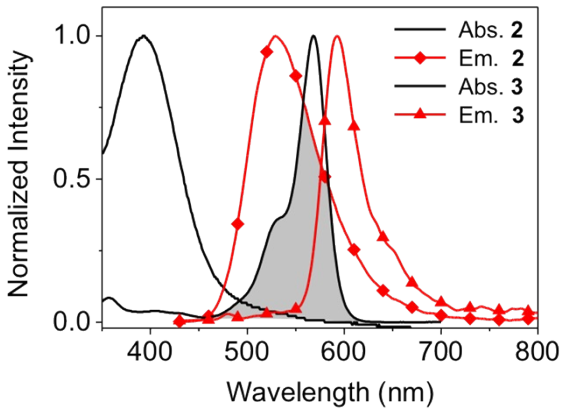

Figure S4. Normalized absorption (Abs.) and emission (Em.) spectra of **2** and **3**. Gray area indicated a spectral overlap between the naphthalimide emission and the rhodamine absorption. All data were obtained in 50 mM buffer solutions containing 1% (v/v) DMSO.

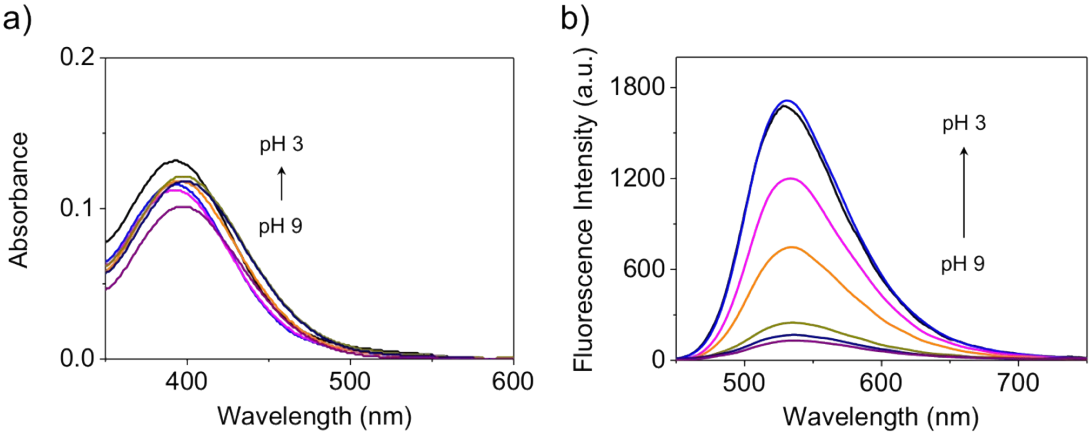

Figure S5. (a) UV/Vis absorption and (b) fluorescence spectra of **2** (10 and 1 μM, respectively) at different pH solutions (3.0, 4.0, 5.0, 6.0, 7.0, 8.0 and 9.0) containing 1% (v/v) DMSO. The excitation was effected at 410 nm.

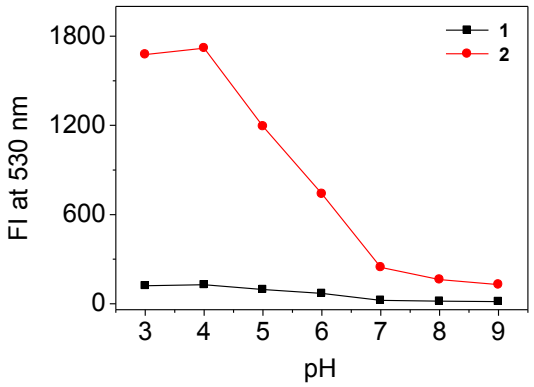

Figure S6. Plot of fluorescence intensities at 530 nm of **1** (1 μM) and **2** (1 μM) *vs* pH. All data were obtained using an excitation of 410 nm at different pH solutions (3.0, 4.0, 5.0, 6.0, 7.0, 8.0 and 9.0) containing 1% (v/v) DMSO.

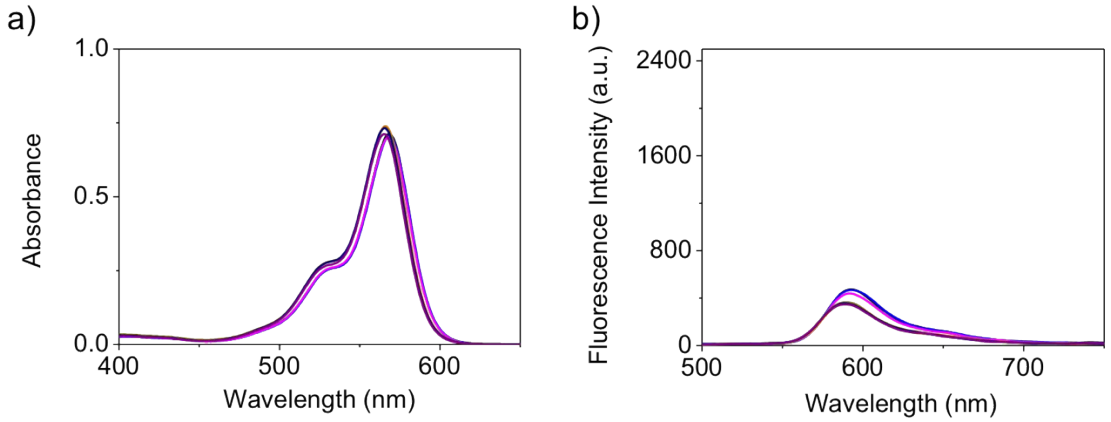

Figure S7. (a) UV/Vis absorption and (b) fluorescence spectra of **3** (10 and 1 μM, respectively) at different pH solutions (3.0, 4.0, 5.0, 6.0, 7.0, 8.0 and 9.0) containing 1% (v/v) DMSO. The excitation was effected at 410 nm.

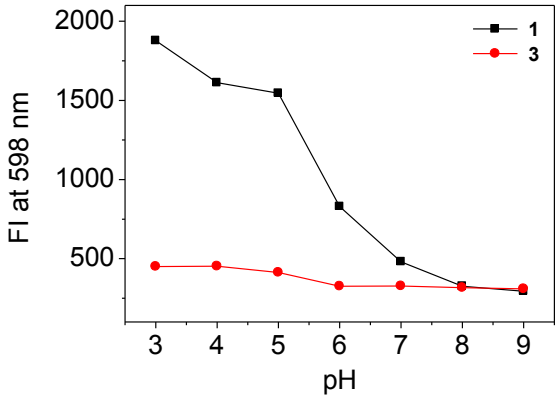

Figure S8. Plot of fluorescence intensities at 598 nm of **1** (1 μM) and **3** (1 μM) *vs* pH. All data were obtained using an excitation of 410 nm at different pH solutions (3.0, 4.0, 5.0, 6.0, 7.0, 8.0 and 9.0) containing 1% (v/v) DMSO.

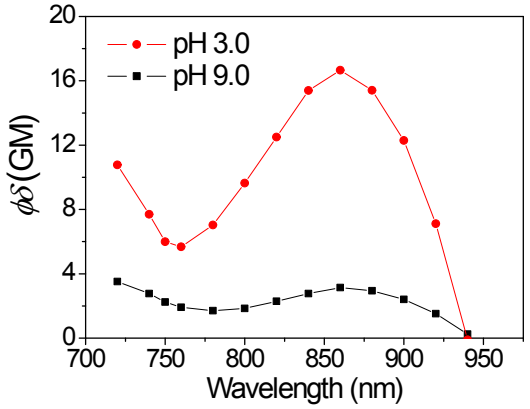

Figure S9. Two-photon action spectra of probe **1** (5 μM) in pH 3.0 and 9.0 buffer solutions containing 10 % (v/v) DMSO. The estimated uncertainties for the two-photon absorption action cross section values (δΦ) are ± 15%.

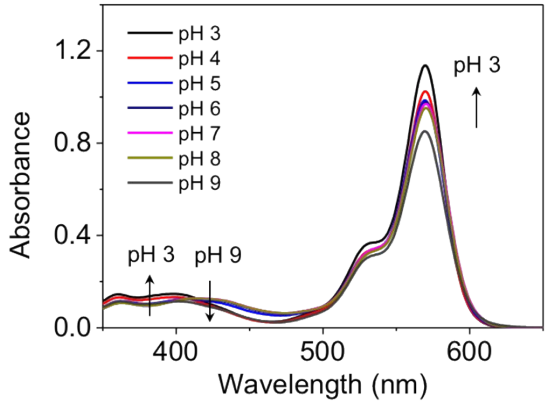

Figure S10. UV/Vis absorption of **1** (10 μM) recorded at different pH values (3.0, 4.0, 5.0, 6.0, 7.0, 8.0, and 9.0). All data were obtained in 50 mM buffer solution containing 1% (v/v) DMSO.

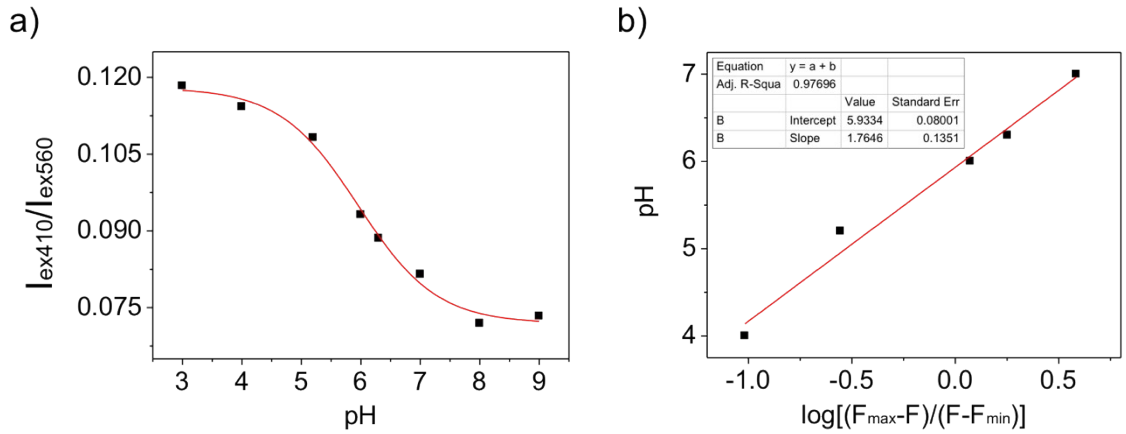

Figure S11. (a) Plot of a ratio (I_{ex410} /I_{ex560}) *vs* pH. The I_{ex410} and I_{ex560} present the fluorescence intensities at 598 nm of **1** recorded using the excitations of 410 and 560 nm, respectively. (b) Plot of pH *vs* log[(F_{max} - F)/(F - F_{min})] using the Henderson-Hasselbach type mass action equation; log[(F_{max} - F)/(F - F_{min})] = p*K*a - pH, where F is the observed fluorescence intensity ratio (I_{ex410} /I_{ex560}) at 598 nm of **1**. The y-intercept is the p*K*a value (5.93 ± 0.08) of **1**.

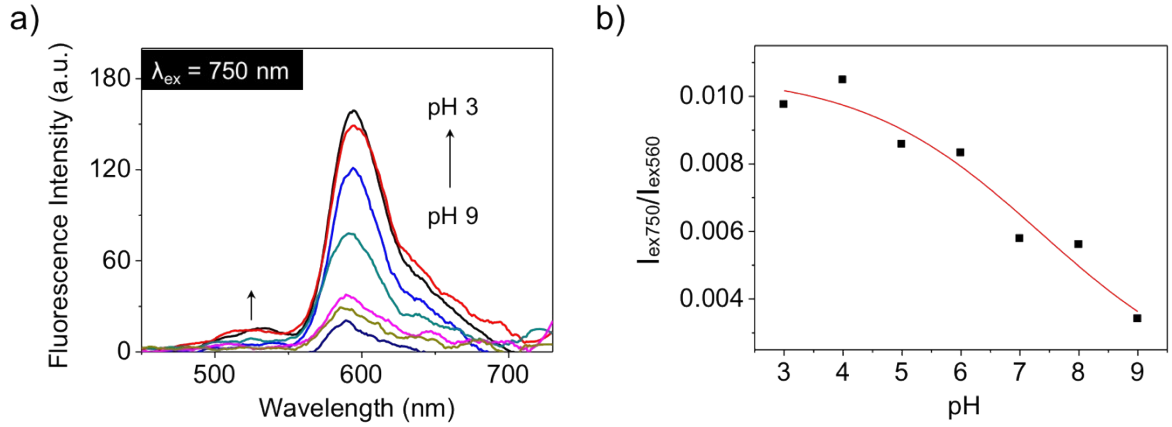

Figure S12. (a) Fluorescence changes of **1** (1 μM) recorded at different pH values (3.0, 4.0, 5.0, 6.0, 7.0, 8.0, and 9.0) using excitation of 750 nm. (b) Plot of a ratio (I_{ex750}/I_{ex560}) *vs* pH. The I_{ex750} and I_{ex560} present the fluorescent intensities at 598 nm of **1** recorded using the excitations of 750 and 560 nm, respectively.

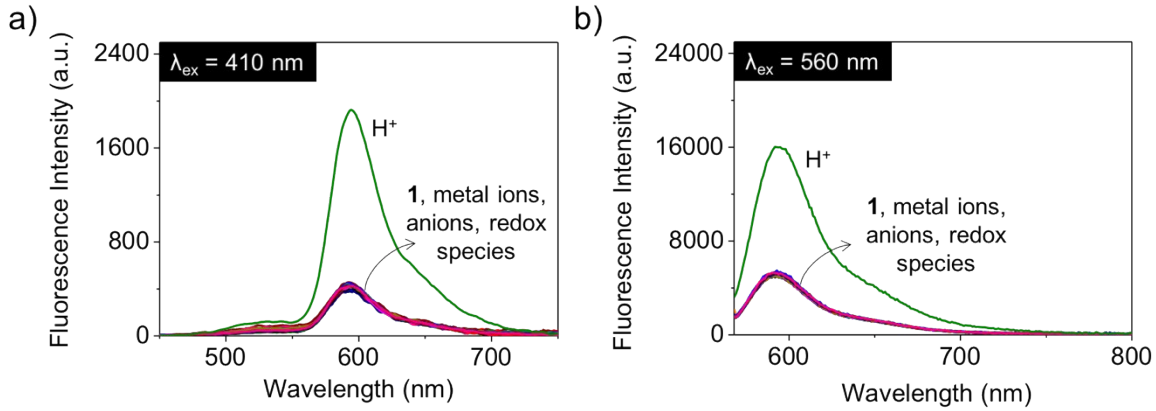

Figure S13. Fluorescence spectra of **1** (1 μM) in the presence of metal ions (Na^+, K^+, Mg^{2+}, Ca^{2+}, Cu^+, Cu^{2+}, Zn^{2+}, Fe^{2+}, Fe^{3+}), anions ($H_2PO_4^-$, AcO^-, OH^-, Cl^-), reactive oxygen species (ClO^-, H_2O_2, $^{\bullet}O_2^-$, $^{\bullet}OH$, $^{t}BuO^{\bullet}$, $^{t}BuOOH$), and thiols (Cys, Hcy, GSH) (10 μM, respectively) and proton (H^+) derived from a pH 3 buffer solution (50 mM) using excitations of (a) 410 and (b) 560 nm. All data were obtained in PBS buffer solution (100 mM, pH 7.4) containing 1% (v/v) DMSO.

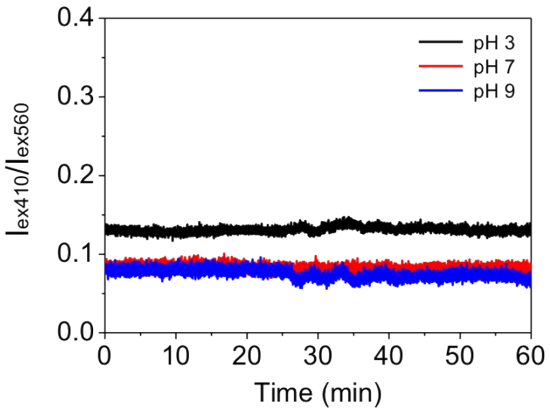

Figure S14. Photostability of **1** (1 μM) at different pH values; pH 3.0 (black line), pH 7.0 (red line) and pH 9.0 (blue line). Plot of a ratio (I_{ex410}/I_{ex560}) *vs* time. The I_{ex410} and I_{ex560} present the fluorescent intensities at 598 nm of **1** recorded using the excitations of 410 and 560 nm, respectively. All data were obtained using excitations of 410 and 560 nm in 50 mM buffer solution containing 1% (v/v) DMSO.

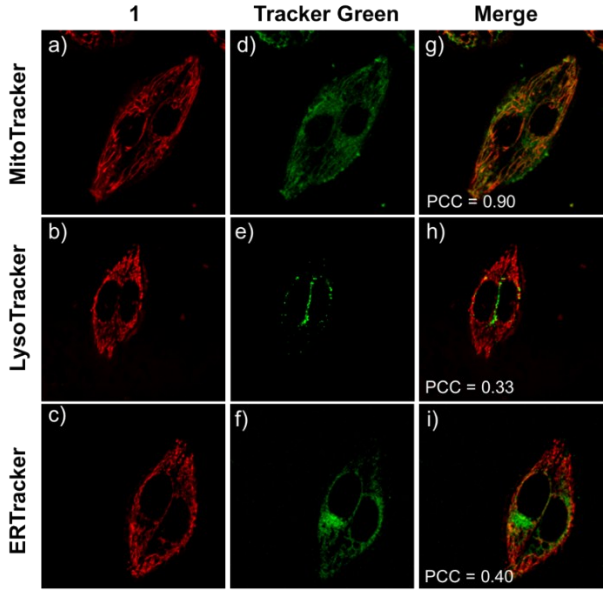

Figure S15. Colocalization experiments using **1**, MitoTracker Green, LysoTracker Green and ERTracker Green in HeLa cells. The cells were incubated with **1** (2 μM) for 15 min at 37 ºC, and the medium was replaced with fresh medium containing Mitotracker Green (0.5 μM), Lysotracker Green (0.3 μM) and ER tracker Green (0.3 μM), respectively and incubated for 15 min. Images for (a–c) **1** and (d–f) tracker Green were then recorded using excitation wavelengths of 543 and 488 nm and band-path emission filters at 585–615 nm and 505–530 nm, respectively. Panels (g–i) show merged images of (a–c) and (d–f).

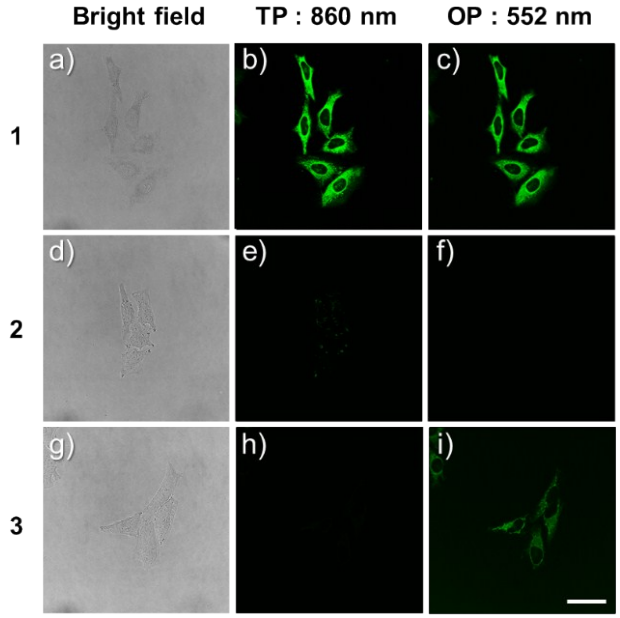

Figure S16. (a, d, g) Bright field images, (b, e, h) TPM and (c, f, i) OPM images of HeLa cells labelled with 5 μM of (a-c) **1**, (d-f) **2** and (g-i) **3**, respectively. The images were acquired with TP (860 nm) and OP (552 nm) excitations, and emission detection window at 550-700 nm, respectively. Scale bar: 40 μm.

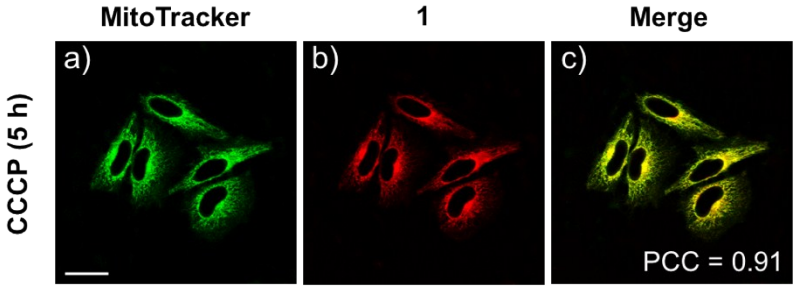

Figure S17. Colocalization image of **1** in CCCP (10 μM) pretreated HeLa cells for 5 h. Cells were treated with (a) MitTracker (500 nM, 15 min) and (b) **1** (2 μM, 15 min). (c) Merged image of (a) and (b). Images were recorded by using excitation wavelengths of 488 nm and 543 nm and detection wavelengths with 505-530 nm band pass (green) and 650 nm long pass (red) filters being employed. Scale bar: 30 μm.

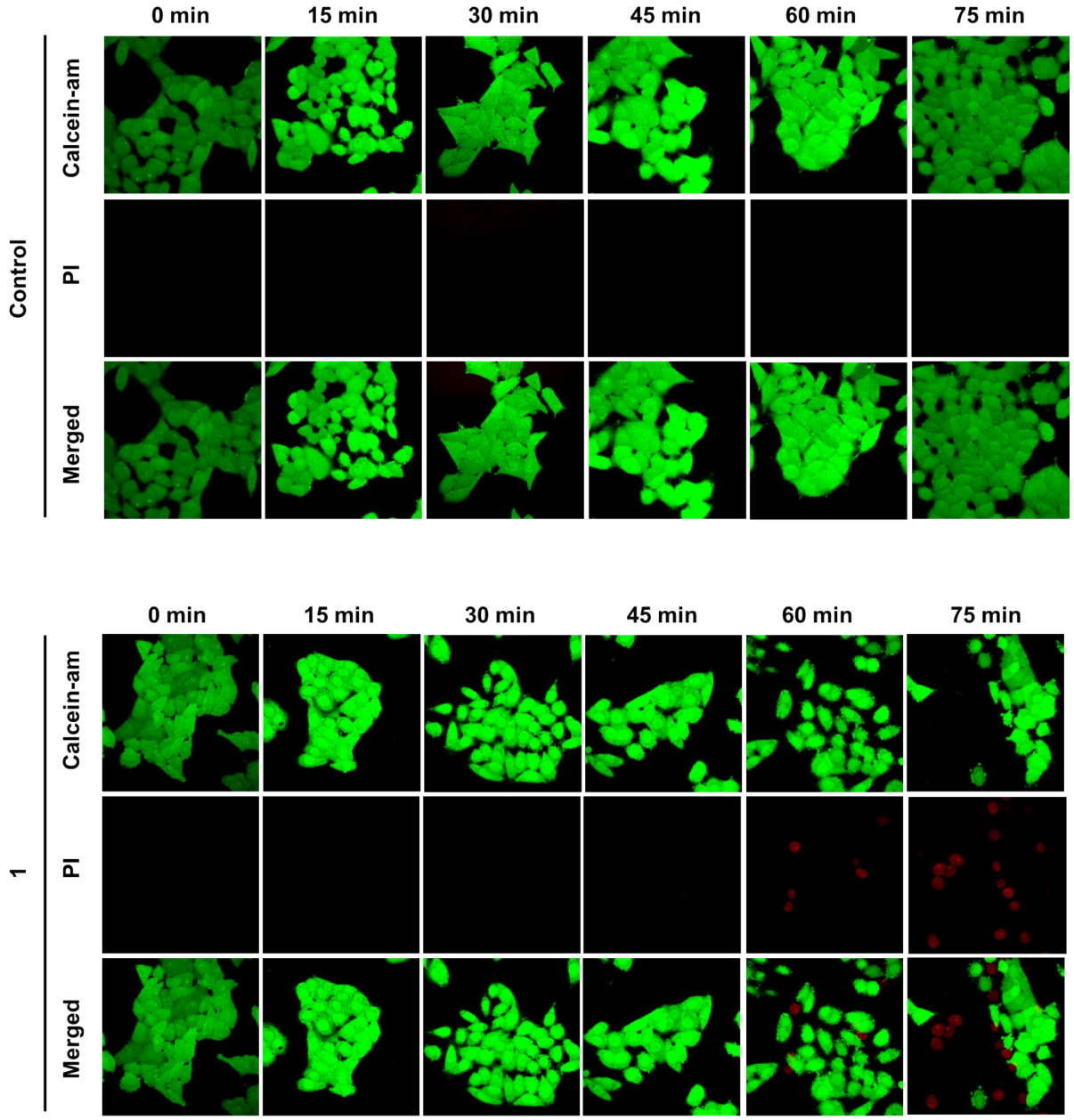

Figure S18. Time course of cell viability experiments using calcein-am and propidinium iodide (PI) without (control) and with **1**. The cells were pre-incubated with **1** (5 μM), calcein-am (1 μM) and PI (100 μM) for 30 min at 37 °C, then recorded from 0 to 75 min using excitation wavelengths of 488 and 633 nm and band-path emission filters at 505–530 nm and 585–650 nm corresponding to calceine-am (green, live cells) and PI (red, dead cells), respectively. Below panels show merged images of calcein-am and PI.

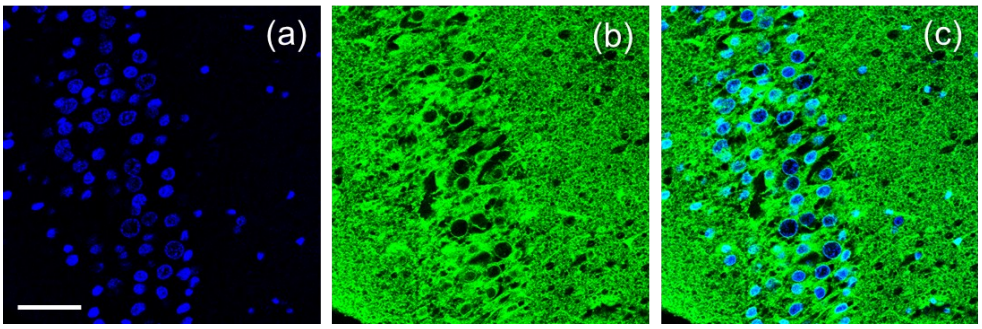

Figure S19. (a-c) TPM images of a rat hippocampal slice co-stained with 10 μM of **1** and 1 μM of **ABI-Nu** (nucleus-staining TP dye) at 400-475 nm (blue) and 550-700 nm (green) at a depth of 120 μm. (c) Merged image of (a) and (c). The TPM images were acquired using excitations of (a) 750 nm and (b) 860 nm, respectively. Scale bar: 40 μm.

References

1. M. H. Lee, *J. Fluoresc*., 2016, **26**, 807–811.
2. D. Oushiki, H. Kojima, T. Terai, M. Arita, K. Hanaoka, Y. Urano and T. Nagano, *J. Am. Chem. Soc.*, 2010, **132**, 2795–2801.
3. T. Förster, *Discuss. Faraday Soc*., 1959, **27**, 7–17.
4. J. R. Lakowicz, *Principles of fluorescence spectroscopy*, Springer Science + Business Media, New York, 3rd edn, 2006.
5. D. W. Brousmiche, J. M. Serin, J. M. J. Frechet, G. S. He, T.-C. Lin, S.-J. Chung, P. N. Prasad, R. Kannan and L.-S. Tan, *J. Phys. Chem. B*, 2004, **108**, 8592–8600.
6. S. K. Lee, W. J. Yang, J. J. Choi, C. H. Kim, S. J. Jeon and B. R. Cho, *Org. Lett.*, 2005, **7**, 323–326.
7. N. S. Makarov, M. Drobizhev and A. Rebane, *Opt. Express*, 2008, **16**, 4029–4047.
8. M. H. Lee, N. Park, C. Yi, J. H. Han, J. H. Hong, K. P. Kim, D. H. Kang, J. L. Sessler, C. Kang and J. S. Kim, *J. Am. Chem. Soc.*, 2014, **136**, 14136–14142.
9. J. H. Kwak, Y. He, B. Yoon, S. Koo, Z. Yang, E. J. Kang, B. H. Lee, S.-Y. Han, Y. C. Yoo, K. B. Lee and J. S. Kim, *Chem. Commun*., 2014, **50**, 13045–13048.